1 # The evolution of micro-cursoriality in mammals

2

3 **Barry, G. Lovegrove and Metobor, O. Mowoe**

4

5 *School of Life Sciences, University of KwaZulu-Natal, Private Bag X01, Scottsville, 3209.*

6 *Email: lovegrove@ukzn.ac.za; m_mowoe@yahoo.co.uk*

7

8 Keywords: Elephant-shrews, Macroscelidae, running speed, cursors, mammals

9

10 Running head: Running speeds of elephant-shrews

11

12 **Abstract**

13

14 In this study we report on the evolution of micro-cursoriality, a unique case of cursoriality in

15 mammals smaller than 1 kg. We obtained new running speed and limb morphology data for

16 two species of elephant-shrews (*Elephantulus* spp., Macroscelidae) from Namaqualand,

17 South Africa, which we compared with published data for other mammals. *Elephantulus*

18 maximum running speeds were higher than most mammals smaller than 1 kg. *Elephantulus*

19 also possess exceptionally high metatarsal:femur ratios (1.07) that are typically associated

20 with fast unguligrade cursors. Cursoriality evolved in the Artiodactyla, Perissodactyla, and

21 Carnivora coincident with global cooling and the replacement of forests with open landscapes

22 in the Oligocene and Miocene. The majority of mammal species, though, remained non-

23 cursorial, plantigrade, and small (< 1 kg). The extraordinary running speed and digitigrady of

24 elephant-shrews was established in the Early Eocene in the earliest macroscelid *Prodiacodon*,

25 but was probably inherited from Paleocene, Holarctic stem macroscelids. Micro-cursoriality

26 in macroscelids evolved from the plesiomorphic plantigrade foot of the possum-like ancestral

27 mammal earlier than in other mammalian crown groups. Micro-cursoriality evolved first in

28 forests, presumably in response to selection for rapid running speeds facilitated by local

29 knowledge, in order to avoid predators. During the Miocene, micro-cursoriality was pre-

30 adaptive to open, arid habitats, and became more derived in the newly-evolved *Elephantulus*

31 and *Macroscelides* elephant-shrews with trail running.

32

33 **List of abbreviations**

34

35 K-Pg: Cretaceous-Paleogene boundary

36 mya: millions of year ago

37 MT: metatarsal

38 F: femur

39 MT:F: metatarsal:femur ratio

40 MRS: maximum running speed (km h^{-1})

41 RRS: relative running speed (body lengths sec^{-1})

42 T_b: body temperature ($^{\circ}$C)

43 OLS: ordinary least squares

44 PGLS: phylogenetic generalized least squares

45 AIC: Akaike information criterion

46 M_b: body mass

47 ML: maximum likelihood

48 CI: confidence interval

49 MANOVA: multivariate analysis of variance

50   **Introduction**

51

52   The extraordinary diversity of modern placental mammals evolved from a single lineage

53   which survived the asteroid impact event that drove the nonneornithean dinosaurs to

54   extinction at the Cretaceous-Paleogene (K-Pg) boundary 65.5 million years ago (mya)

55   (O'Leary et al., 2013). The ancestral placental mammal was a small (6 - 245g), insectivorous,

56   tree-climbing (scansorial), forest-dweller, which looked somewhat like an opossum with a

57   bushy tail (O'Leary et al., 2013). The reconstruction of this virtual placental mammalian

58   ancestor shows the ancestral condition of a plantigrade foot, in which the heel makes contact

59   with the ground (O'Leary et al., 2013). From this ancestor, and given the freedom to radiate

60   into niches evacuated by the nonneornithean dinosaurs, the first members of the modern

61   placental mammals emerged within hundreds of thousands of years of the extinction event

62   (O'Leary et al., 2013). During the Oligocene and Miocene, a high degree of cursoriality

63   evolved in several modern placental orders (Carnivora, Artiodactyla, and Perissodactyla) in

64   response to the emergence of open landscapes and grasslands following the Eocene Thermal

65   Maximum (Janis, 1993; Janis and Wilhelm, 1993; Yuanqing et al., 2007; Jardine et al., 2012;

66   Lovegrove, 2012b; Lovegrove and Mowoe, 2013).

67   Loosely defined, cursorial mammals are those that run fast. However, more explicit

68   definitions of cursoriality remain obscure because locomotor performance is influenced by

69   multiple variables, including behaviour, biomechanics, physiology, and morphology (Taylor

70   et al., 1970; Garland, 1983a, b; Garland and Janis, 1993; Stein and Casinos, 1997; Carrano,

71   1999). In an evaluation of these definition problems, Carrano (1999) argued that

72   "…morphology should remain the fundamental basis for making distinctions between

73   locomotor performance…" (Carrano, 1999). Carrano (1999) showed that a morphological

74   continuum between "cursorial" and "graviportal" (weight-bearing) locomotion based upon

75   measures of multiple morphological traits in an principal components analysis provided

76   biologically realistic indices of mammalian locomotor performance. In short, cursorial taxa

77   have longer metatarsals, more slender limb elements, shorter femora, and a muscle insertion

78   point located closer to the hip joint, whereas graviportal mammals have more robust limb

79   elements, shorter metatarsals, and more distal muscle insertion points (Carrano, 1999).

80   Variations in the dimensions of these traits are borne in limbs commonly associated

81   with cursoriality, namely the derived digitigrade and unguligrade limbs, in which the

82   metatarsals, in particular, are elongated relative to other hindlimb bones, resulting in the heel

83   being raised off the ground (Hildebrand, 1974; Garland and Janis, 1993). The length ratio

84 between the metatarsals (MT) and the femur (F), the MT:F ratio, is often used as a proxy for

85 cursoriality in mammals (Garland and Janis, 1993; Carrano, 1999). Although higher MT:F

86 ratios are often associated with increased hindlimb length, stride length and running speed

87 (Hildebrand, 1974), they are also indicative of more specialized limb adaptations for fast

88 running speeds (Steudel and Beattie, 1993) and cost-effective long-distance locomotion

89 (Garland and Janis, 1993). Nevertheless, there is no direct relationship between MT:F ratio

90 and maximum running speed; two mammals with similar body sizes can have similar

91 maximum running speeds but very different MT:F ratios (Garland and Janis, 1993). MT:F

92 ratios range from < 0.1 in some plantigrade rodents to 1.4 in the giraffe (Carrano, 1999).

93   Several published observations on the morphology and physiology of elephant-shrews

94 or sengis (Macroscelidea) prompted us to test the hypothesis that elephant-shrews are

95 exceptional micro-cursors relative to typical cursors. Elephant-shrews are placed in the

96 superorder Afrotheria (Springer et al., 1997) as a sister family to Afrosoricida (tenrecs,

97 golden moles and otter shrews) (Stanhope et al., 1998). The etymology of Macroscelidea

98 confirms the early recognition of unusual hind limb morphology because the word is derived

99 from *Macroscelides* comprised of the Latin prefix "*macro*" meaning large, and the Greek

100 word "*skelis*", meaning hip or thigh. Indeed, elephant-shrews that have been studied

101 morphologically to-date display extremely elongated metatarsals and distal muscle reductions

102 (Evans, 1942; Carrano, 1999). Moreover, whereas their closest relatives, tenrecs (Tenrecidae)

103 and golden moles (Chrysochloridae), display a mean body temperature (T_b) of 32.8^oC (n = 8

104 species), the mean T_b of elephant-shrews is 37.2^oC (n = 8 species), indicating a profound

105 apomorphy (derived characteristic) of 4.4^oC between sister Afrotherians (Lovegrove, 2012a;

106 Lovegrove, 2012b) (see Fig. 1, supplementary information). High body temperatures are

107 correlated with the MT:F in other cursors (Lovegrove, 2012b), and are thought to enhance

108 muscle performance (Clarke and Pörtner, 2010). Elephant-shrews also display an

109 exceptionally high MT:F ratio for their body size, comparable to those of the fastest

110 unguligrade cursors (Lovegrove, 2012b). Last, elephant-shrews (*Elephantulus*) displayed the

111 highest index of cursoriality in a principal components analysis of mammal limb dimensions

112 (Carrano, 1999).

113   The extraordinary large hind limbs/quarters and speed of elephant-shrews were also

114 recognized in the very first written description of these African small mammals an annotation

115 that accompanied a drawing now thought to have been that of *Macroscelides proboscideus*

116 (Rookmaker, 1989). It was recorded during the fourth journey into the northwestern Cape of

117 South Africa by Robert Jacob Gordon on 02 August 1779;

118

119 "*Door mij, oliphantsmuis genaamt, om sign lange snuit dewelke hij op allerley manieren*

120 *bewegen kan, sijn voorpoten veel korter als de agterpoten. Is egter seer geswind in het*

121 *lopen,…*"

122

123 The English translation reads;

124

125 "By me, called *oliphantsmuis* (elephant mouse), for the long snout which can be moved in

126 many ways. Its front legs much shorter than the hind ones. It is very fast…"

127

128 The limbs and other unique characteristics of elephant-shrews (exposed shelter sites, mixed

129 herbivory and insectivory, social monogamy, small precocial litters, and small body size < 1

130 kg), have been described as "the micro-cursorial adaptive syndrome" (Rathbun, 1979, 2009).

131 Two ecologically relevant measures of running speed; maximum running speed

132 (MRS; km/h), and relative running speed (RRS, body lengths/s) have been used in the

133 literature (Van Damme and Van Dooren, 1999; Iriarte-Diaz, 2002). On average, large

134 mammals display higher MRSs than small mammals (Garland, 1983a), whereas small

135 mammals display higher RRSs than large mammals (Steudel and Beattie, 1993; Iriarte-Diaz,

136 2002). The regression of RRS as a function of body mass (M_b) has a negative slope, and

137 displays an inflection at a M_b of ~ 500 g, i.e. the negative slope of the regression for

138 mammals larger than 500 g is steeper, which the authors suggest confirms that RRS decreases

139 more rapidly with increasing body size (Iriarte-Diaz, 2002). However, although we accept the

140 concept of relative running speed as a notable ecological consideration, the allometric scaling

141 patterns that have been reported and which quantify RRS are questionable because two body-

142 size related variables (log body lengths.s^{-1} and M_b) were regressed against each other (Iriarte-

143 Diaz, 2002). Consequently, we resorted here to analyses of MRS only, using a

144 phylogenetically-informed approach.

145 In this study we measured the running speeds and limb morphology of two species of

146 rock elephant-shrew, *Elephantulus edwardii* and *E. rupestris,* from Namaqualand, South

147 Africa. We recorded the MT:F ratio and maximal running speed (km.h^{-1}) and compared these

148 data with appropriate mammal models for which running speed and MT:F data were

149 available. We tested the hypothesis that elephant-shrews display a micro-cursorial capacity

150 which evolved in forest environments with some surety during the Early Eocene, but possibly

151 as early as the Paleocene.

152

153   **Results**

154

155   *Metatarsal:femur ratios*

156   The average metatarsal:femur ratio of the two species of *Elephantulus* was 1.07 (Table 1).

157   Excluding the giraffe, only five mammals in the combined dataset of 135 mammals had

158   MT/F ratios higher than those of the *Elephantulus* species (3 *Gazella* spp., the dik dik

159   *Madoqua kirkii*, and the springbok *Antidorcas marsupialis*) (Fig. 1). No mammal smaller

160   than 1 kg, apart from *Elephantulus*, showed a MT:F ratio > 0.7 (Fig. 1). A statistical

161   comparison of the MT:F ratios of *Elephantulus* with those of other mammals is quite

162   unnecessary because the data for *Elephantulus* are so markedly higher than those of other

163   similar-sized mammals (Fig. 1). Nevertheless, we report the results of the ordinary least

164   squares (OLS) and the phylogenetic generalized least squares (PGLS) models fitted to the

165   data because they bear relevance to previous studies which found no significant allometric

166   relationships.

167   The OLS and PGLS regressions of MT:F ratio as a function of $\log_{10}M_b$ of the

168   complete dataset (n = 135) were significant (Table 2). However, whereas the slope of the

169   OLS regression was positive, i.e. indicating an increase in MT:F ratio with body size (not

170   shown in Fig. 1), those of the phylogenetic regressions were negative, consistent with the

171   negative slopes for the separate unguligrade and non-unguligrade regressions (see below).

172   Thus the positive slope of the OLS regression, plus the large values of ΔAIC > 200 between

173   the OLS and the PGLS regressions, render the OLS regression meaningless. The PGLS with

174   maximum likelihood (ML) estimation showed the best fit to the data (Fig. 1, red line) and

175   also showed significant phylogenetic signal [$\lambda = 0.964$, significantly different to both $\lambda = 0$,

176   lower 95% confidence interval (CI) = 0.901, and $\lambda = 1$, upper 95% CI = 0.997] close to, but

177   not quite equal to, a Brownian motion evolutionary model (Table 2).

178   There was significant phylogenetic signal for both M_b and residual MT:F ratio in

179   the unguligrade and non-unguligrade datasets (Table 3). The best fitting regression models

180   for the 56 species of unguligrade mammal were the two PGLS regression (ΔAIC = 54.9

181   compared with the OLS regression) which both indicated a Brownian motion model of

182   evolution ($\lambda = 1$, Table 2, Fig. 1). For the 79 non-unguligrade mammals, the PGLS with ML

183   estimation provided the best fit to the data (Fig. 1) and confirmed significant phylogenetic

184   signal ($\lambda = 0.589$, lower 95% CI = 0.279, upper 95% CI = 0.819, Table 2). The slope of the

185 unguligrade PGLS regression (-0.124) was steeper than that of the non-unguligrade PGLS

186 regression (-0.031) (Table 2, Fig. 1).

187

188 *Maximum running speed model*

189 The mean MRSs of *E. rupestris* and *E. edwardii* were 23.6 km/h and 19.4 km/h, respectively

190 (Table 1). The fastest individual run recorded was 28.8 km/h by a female *E. ruprestris*.

191 Piecewise regression identified a significant inflection in the regression of $\log_{10}$ MRS

192 as a function of $\log_{10}$ M_b of 143 species of mammals (excluding *Elephantulus* spp.) ranging in

193 M_b from 9 g (*Perognathus longimembris*) to 6,000 kg (*Loxodonta africana*) (Fig. 2). The

194 inflection occurred at a body mass of 20 kg. The largest mammal in the small mammal data

195 set was the Cape hunting dog (*Lycaon pictus*). The 80 species < 20 kg were comprised of 49

196 rodents, 8 lagomorphs, 12 marsupials, 10 carnivores and one artiodactyal (*Madoqua kirkii*).

197 Both $\log_{10}$ M_b and residual $\log_{10}$ MRS showed significant phylogenetic signal as detected by

198 Blomberg et al.'s (2003) *K* estimate (Table 3).

199 In the significant OLS regression of the small mammal data there were no outliers,

200 that is, no studentized residuals > 3 (Jones and Purvis, 1997) or Cook's Distance *D* values >

201 0.5. Four of the five species with the highest studentized residuals were lagomorphs, whereas

202 those with the lowest residuals were the ground hog *Marmota monax*, the striped skunk

203 *Mephitis mephitis*, and the western pygmy possum *Cercatetus concinnus*.

204 The presence of so many lagomorphs with high MRS residuals suggested that there

205 may be differences in the MRS between the four locomotor modes. A non-PGLS multivariate

206 MANOVA confirmed a significant effect of locomotor mode on MRS (Table 4). We omitted

207 the solitary unguligrade datum (*Madoqua*) from the multivariate MANOVAs of the small

208 mammal dataset because of sample size. Once corrected for phylogenetic effects, the PGLS

209 multivariate MANOVA showed no significant influence of locomotor mode on MRS (Table

210 4). Thus the model against which the elephant-shrew MRSs were initially compared was

211 comprised of 80 mammals smaller than 20 kg which included all locomotor modes

212 (plantigrade, digitigrade, lagomorph-like, and saltatorial), but excluded the solitary

213 unguligrade datum for *Madoqua*. Both body mass and residual MT:F ratio in this dataset

214 showed significant phylogenetic signal (Table 3).

215 The phylogenetic PGLS Brownian motion regression model of the small mammal

216 data was significant and its AIC value was lower than that of the OLS regression (ΔAIC =

217 18.88, Table 5). Thus a Brownian motion evolutionary model provided a considerably better

218 fit to the data than a model that assumed no phylogenetic structure (star phylogeny).

219   However, the evolutionary model with the lowest AIC, and hence the best fit of the models,

220   was the PGLS model in which the branch length transformations were estimated with Pagel's

221   *lambda* ($\lambda = 0.905$, significantly > 0, lower 95% CI = 0.699, and < 1, upper 95% CI = 0.988,

222   Table 5), confirming significant phylogenetic signal. To our knowledge, there is no way of

223   fitting 95% confidence and prediction intervals to a PGLS regression with ML estimated

224   branch length transformations that would allow a comparison of the MRS of elephant-shrews

225   with those of mammals smaller than 20 kg.

226   We resorted instead to fitting the 95% confidence and prediction intervals to a

227   Brownian motion PGLS, which is equivalent to fitting an OLS to the phylogenetically

228   independent linear contrasts (Blomberg et al., 2012) (Fig. 3). In this graphical representation,

229   the most obvious observations were that a) the MRS of 7 of the 8 lagomorphs lay above the

230   upper 95% confidence interval, and b) the digitigrade mammals and lagomorphs showed a

231   marginal body size overlap with the plantigrade mammals (non-sciurids rodents, sciurids, and

232   marsupials); three squirrels and a primate did overlap. Thus, as stated earlier, a lack of body

233   overlap obviates a comparison of the MRSs of elephant-shrews with digitigrade mammals

234   and carnivora. The data for *Elephantulus* lay above the regression line, but not above the 95%

235   confidence intervals (Fig. 3).

236   There were 52 species in the plantigrade database that were smaller than 0.5 kg (44

237   rodents and 8 marsupials). Interestingly, there was no significant phylogenetic signal for

238   residual $\log_{10}$ MRS using both Blomberg et al.'s (2003) *K* estimate, as well as Pagel's ML

239   lambda which was not significantly different to 0 (p = 1), but significantly different 1 (p <

240   0.001). Not surprisingly, the OLS of the MRS of these mammals was significant, but none of

241   the PGLS models showed significance. When the data for *Elephantulus* were mapped back

242   onto the OLS regression, the datum for *E. rupestris* lay above both the 95% confidence and

243   prediction intervals, indicating a significantly higher MRS than other plantigrade small

244   mammals (Fig. 4). The two larger species with absolute MRSs slightly higher than that of *E.*

245   *ruprestris* were the marsupial *Dasyuroides byrnei*, and the squirrel, *Sciurus carolinensis*.

246

247   **Discussion**

248

249   *MT:F ratios*

250   Although it was not a specific objective of this study to evaluate the allometry of

251   MT:F ratios, the results of our analyses are noteworthy. Garland and Janis (1993) analyzed

252   the MT:F ratio allometry in 49 mammal species, 30 ungulates and 19 carnivores, and found

253   no significant phylogenetically-corrected relationship between MT:F ratio and $\log_{10}M_b$ in any

254   of their regressions (complete dataset, ungulates, carnivores). In our expanded, more

255   taxonomically diverse dataset (n = 135 species), all of our phylogenetically-corrected

256   regressions showed significant allometries of MT:F ratio and $\log_{10}M_b$. With the exception of

257   the *Elephantulus* data, the data fall neatly into either the unguligrade or non-unguligrade

258   distributions. Although we did not test for interordinal differences within the non-unguligrade

259   mammals, it would seem that carnivores and lagomorphs, for example, both considered to be

260   cursorial, do not display MT:F ratios obviously different from other non-unguligrade

261   mammals, such as primates and non-macropod marsupials, that are considered to be non-

262   cursorial.

263   These data emphasize that the MT:F ratio of mammals smaller than 1 kg never

264   exceeds 0.7, whereas it does in larger unguligrade mammals. Thus cursoriality never evolved

265   in the majority of mammals, that is, those smaller than 1 kg (see Lovegrove and Mowoe,

266   2013). On the other hand, the rates of evolution of cursoriality as measured by the MT:F ratio

267   accelerated during the Oligocene and Miocene in typical large-bodied herbivorous cursors

268   (Garland and Janis, 1993; Janis and Wilhelm, 1993).

269   The negative slope of the allometry for unguligrade mammals that we report here can

270   probably be attributed to the continuum of morphological traits along the cursorial-

271   graviportal continumm (Carrano, 1999). In terms of fitness, longer metatarsals, more slender

272   limb elements, shorter femora, and muscle insertion points located closer to the hip joint

273   evolved in the smallest unguligrade mammals because weight bearing was less important

274   than maximum running speed. Consequently, small ungulates also have a higher maximum

275   running speed than big ungulates (Garland, 1983a; Lovegrove, 2004).

276   The allometry of the non-unguligrade mammals is hardly worthy of mention because

277   the slope of the best-fit regression is so low despite being significantly different from zero.

278   Moreover, there seems to be no consistent taxonomic trend in MT:F ratios in these data. For

279   example, the species with the top 10 highest ratios (0.490 – 0.649) include six rodents, one of

280   which is saltatorial (*Dipodomys*), the saltatorial marsupial *Bettongia penicullta*, one

281   lagomorph, *Lepus americanus*, one lipotyphlan, *Sorex cinereus*, and one carnivore, *Felis*

282   *nigripes*.

283   We offer one explanation for the difference in the MT:F ratio of similar-sized

284   unguligrade and non-unguligrade mammals; the evolutionary tradeoff between locomotor

285   performance and digit functionality (Lovegrove and Mowoe, 2013). The tradeoff posits that

286   the fitness benefits of unguligrady in herbivores far outweighed the fitness costs of the loss of

287   digit numbers and functionality, which was not the case in carnivores (Lovegrove and

288   Mowoe, 2013). The divergence in MT:F ratios occurred in the Oligocene and Miocene when

289   there was a dramatic acceleration in the rate of evolution of the MT:F ratio in herbivores, but

290   not in carnivores (Garland and Janis, 1993; Janis and Wilhelm, 1993), despite the fact that

291   both herbivores and carnivores were also increasing in body size (Lovegrove and Mowoe,

292   2013).

293   Relative to other similar-sized mammals, elephant-shrews, such as *E. ruprestris*,

294   display remarkable digitigrade-like adaptations of the limbs. The metatarsal:femur ratios of

295   the elephant-shrews were more than double the average for 24 other species (0.42) of small

296   mammals < 1 kg, but were comparable with some of the highest of all mammalian ratios,

297   namely those of the cursorial Artiodactyla > 1 kg. *Elephantulus* elephant-shrews also

298   displayed maximum running speeds faster than those of all mammals smaller than 1 kg,

299   except for a larger squirrel and a marsupial. These fast running speeds can undoubtedly be

300   attributed to the digitigrady of *Elephantulus* as quantified by their very high MT:F ratios for

301   such small mammals. No other mammal smaller than 1 kg has a MT:F which exceeds 0.7.

302   Thus elephant-shrews are not only the smallest mammalian cursors, they can also run faster

303   than the majority of mammals smaller than 1 kg.

304

305   *Maximum running speeds*

306   In absolute terms, the MRSs of elephant-shrews were comparable with those of larger

307   digitigrade carnivores, but they were not as fast as lagomorphs, although these differences

308   could not be quantified or tested statistically. Nevertheless, these observations, as well as the

309   observation of comparatively slow MRSs in plantigrade mammals smaller than 1 kg

310   (Lovegrove, 2004), supports several hypotheses on the relationship between the evolution of

311   limb morphology and body size in mammals during the Cenozoic (Lovegrove, 2000, 2001,

312   2004; Lovegrove and Haines, 2004; Lovegrove, 2012b; Lovegrove and Mowoe, 2013). For

313   example, the Bowtie Model argued that, following the evolution of larger, faster digitigrade

314   carnivores following the Eocene Thermal Maximum, most plantigrade mammals were

315   constrained from evolving to body sizes larger than ~ 0.5 kg (Lovegrove, 2000, 2001;

316   Lovegrove and Mowoe, 2013). Exceptions occurred with the evolution of body armour,

317   arboriality, an aquatic lifestyle, or exceptionally fast running speeds, such as occurs in the

318   lagomorpha (Garland, 1983a; Lovegrove, 2001). But elephant-shrews are somewhat

319   enigmatic in terms of these mammalian generalizations concerning body size and running

320 speed because they are the only mammals in which digitigrady and high running speeds, that

321 is, micro-cursoriality, evolved in small mammals.

322

323 *The evolution of micro-cursoriality in elephant-shrews*

324 The evolution of widespread cursoriality, especially unguligrady, was driven by Cenozoic

325 cooling and the appearance of more open landscapes and C_4 grasslands following the Eocene

326 Thermal Maximum (ca. 55 mya), especially during the Miocene (Janis and Wilhelm, 1993;

327 Edwards et al., 2010; Figueirido et al., 2012; Lovegrove, 2012b; Secord et al., 2012;

328 Lovegrove and Mowoe, 2013). Moreover, during the Late Cenozoic, both unguligrade and

329 digitigrade mammals showed body size increases (Alroy, 1998; Smith and Lyons, 2011;

330 Lovegrove and Mowoe, 2013) and increased hypsodonty in unguligrade mammals

331 (MacFadden, 2000; Jardine et al., 2012). Nevertheless, although unguligrady and digitigrady

332 were synonomous with several crown orders (Carnivora, Artiodactyla, Perissodactyla), the

333 most common condition remained plesiomorphic plantigrady (Lovegrove and Mowoe, 2013).

334 During the dramatic radiation of the mammals within several 100,000 years of the T-Pg

335 boundary (O'Leary et al., 2013), the evolution of digitigrady occurred surprisingly quickly in

336 "condoylarths" (e.g. Phenacodontidae), ancestral lagomorphs (e.g *Gomphos*), and perhaps the

337 Macroscelidea.

338   Understanding the evolution of micro-cursoriality in elephant-shrews is complicated

339 by uncertainty in the phylogenetic relationships between the Macroscelidea and North

340 American "condylarths" (Aphelescidae, Louisinidae, Amphilemuridae and Adapisoridae)

341 (Zack et al., 2005b; Zack et al., 2005a; Hooker and Russell, 2012; O'Leary et al., 2013).

342 Based upon cladistic analyses, Hooker & Russel (2012) argued that the Macroscelidea

343 evolved from Paleocene, Holarctic "condylarths", many of which, they argue, are basal

344 macroscelideans (Fig. 5) (Zack et al., 2005b; Hooker and Russell, 2012). They suggested

345 placing Aphelescidae within Macroscelidea, together with Louisinidae, Amphilemuridae and

346 Adapisoridae. They dated the basal divergence of the Macroscelidea to the K-Pg boundary ~

347 65 mya (Fig. 5) (Hooker and Russell, 2012).

348   On the other hand, both O'Leary et al.'s (2013) combined phenomic/genomic

349 phylogeny and Zack et al's. (2005b) phylogeny, consider *Apheliscus* (Aphelescidae) to be a

350 North American ungulate basal to Euungulata (= crown Perrisodactyla and Artiodactyla).

351 Rare postcranial skeletons show cursorial specializations of the femur, tibiofibula (distal

352 synostosis, Fig. 6), and the crus of the Paleocene apheliscines *Apheliscus* and *Haplomylus*

353 (Zack et al., 2005b). Tibiofibular synostosis, in particular, is associated with enhanced

354 parasagittal, cursorial capacity (Zack et al., 2005b). The *Apheliscus* fossil is dated at 55.8

355 mya and the split of Aphelescidae with Hyopsodontidae at 63.3 mya (O'Leary et al., 2013).

356 Interestingly, *Hyopsodus* (Hyopsodontidae) had a long dachshund-like body with short legs

357 and no morphological evidence of cursorial capacity (Zack et al., 2005b). However, other

358 closely related families, such as Phenacodontidae and Didolodontidae, tended towards

359 digitigrade cursoriality (Thewissen, 1990), so the possibility that the ancestral euungulate

360 "condylarth" may have been digitigrade cannot be ruled out. The point we wish to emphasize

361 here is that the Early Eocene origin of *Apheliscus*, as well as the questionable phylogenetic

362 placement of the Aphelescidae, does not detract from the development of our argument for an

363 Early Eocene or perhaps even a Paleocene origin of micro-cursoriality in Macroscelidea.

364   There seems to be agreement that the Leptictidae, which were small, insectivorous

365 saltatorial (jumping) and/or cursorial mammals, are the sister clade to Macroscelidea (Hooker

366 and Russell, 2012; O'Leary et al., 2013) (Fig. 5). The hindlimbs of *Leptictis* and *Leptiptidium*

367 show a degree of fibiotibular fusion (Rose, 1999, 2006) that is remarkably similar to the

368 condition in modern elephant shrews, for example *Rhynchocyon* (Zack et al., 2005b) and

369 *Elephantulus* (this study) (Fig. 6). Thus we need to ask whether micro-cursoriality was

370 derived independently in the Macroscelidea and Leptictidae, or whether it was inherited from

371 a common Early Paleocene ancestor.

372   The date of the oldest leptictid, *Prodiacodon crustuluam,* cannot be separated from

373 that of the Afrotherian origin or the Early Paleocene split between the Leptictidea and the

374 Macroscelidea, *ca*. 65 mya (Fig. 5) (O'Leary et al., 2013). Thus if micro-cursoriality was an

375 inherited trait in the macroscelid and leptictid lineages it would have evolved in the Early

376 Paleocene, very soon after the K-Pg extinction event. However, the postcrania of

377 *Prododiacodon* show fusion of the tibia and fibula at the distal end only, "…well below

378 midshaft…", indicating an ancestral synostostic condition (i.e. non-cursorial hindlimb)

379 compared with Eocene leptictids (Rose, 2006). Thus in the leptictid lineage, micro-

380 cursoriality seems to have evolved for the first time in the Eocene.

381   The oldest macroscelid is thought to be *Chambius kasserinensis* (late Early Eocene,

382 Tunisia) estimated to have weighed ~ 13 g (Tabuce et al., 2007). Postcranial remains indicate

383 micro-cursoriality (Tabuce et al., 2007). For example, the pulley-shape and the semicircular

384 crests of the astragalar trochlea, and the calcaneus lengthened proximally and distally to

385 subtarsal joints, are characteristics of fast running speeds and lateral stability (Tabuce et al.,

386 2007). However, without postcranial data for stem macroscelids, the origin of micro-

387 cursoriality in macroscelids cannot at present be reliably dated to earlier than the Early

388 Eocene.

389 Prior to the flourishing of the Paleocene archaic mammals (Alroy, 1998; Yuanqing et

390 al., 2007), some of which attained very large body sizes (Alroy, 1998; Alroy et al., 2000), the

391 earliest Paleocene mammals were *de facto* small-bodied forest dwellers. Small body sizes

392 were retained by macroscelids into the Eocene, as discussed for *Chambius*. Thus the

393 macroscelids show the first appearance of micro-cursoriality in a crown Eutherian order

394 (Tabuce et al., 2007). It is estimated that the two subfamilies of elephant shrews,

395 Macroscelidinae (*Elephantulus*, *Petrodromus* and *Macroscelides*), and Rhynchocyoninae

396 (*Rhynchocyon*), diverged 26 - 43 mya from a forest-adapted ancestor (Douady et al., 2003;

397 Smit et al., 2011).

398 The Rhynchocyoninae speciated ~ 8 - 10 mya coincident with Miocene forest

399 fragmentation induced by aridification (Smit et al., 2011) (Fig. 5). The four recognized

400 species of *Rhynchocyon* are forest dwellers (Rathbun, 2009). Speciation within

401 Macroscelidinae commenced ~ 11.5 – 21. mya following dispersal from east Africa to south-

402 western Africa driven by the aridification of the Sahara and the creation of sub-Saharan arid

403 corridors, and the emergence of savannas and C_4 grasslands (Fig. 5) (Douady et al., 2003;

404 Rathbun, 2009; Smit et al., 2011). The Macroscelidinae display more derived cursorial

405 specializations than *Rhychocyon*, such as a near two-fold increase in the MT:F ratio (Table 6,

406 Fig. 1) and smaller body sizes (< 300 g). In the new open African landscapes, predatory

407 pressures intensified with the influx of modern Carnivora ~ 30 mya when Africa docked with

408 Europe and Asia (Hedges, 2001). Micro-cursoriality was presumably pre-adaptive in newly

409 emerging open landscapes with less canopy cover and shelter provided by trees, which

410 undoubtedly also elevated avian predation. The presence of larger, faster carnivores and avian

411 predators may have placed upper constraints on the body sizes of the macroscelilidids

412 resulting in the evolution of their smaller sizes (Lovegrove, 2001; Lovegrove and Mowoe,

413 2013). Smaller body sizes require lower total energy demands and smaller home ranges, thus

414 reducing daily movement distance requirements and the risk of predation (Garland, 1983a;

415 Van Damme and Van Dooren, 1999; Blanckenhorn, 2000; Lovegrove, 2001). The

416 establishment of a system of maintained trails along which the Macroscelidinae run at great

417 speed also evolved with body size reduction and more open habitats (Rathbun, 2009).

418 Like other cursors (Lovegrove, 2012b), the elevated body temperatures of elephant-

419 shrews relative to their Afrotherian sister clades (Tenrecidae and Chrysochloridae) are

420 thought to be linked with cursoriality and the proposed temperature dependence of muscle

421 performance (Clarke and Pörtner, 2010). Selection for T_b tending towards supraendothermy

422 ($T_b > 37.9^\circ$C) (sensu Lovegrove, 2012a) presumably continued until the fitness benefits of

423 enhanced locomotor capacity were balanced by the costs of the increased metabolic demands

424 associated with micro-cursoriality. However, in small Macroscelilinae, that is, those with the

425 highest mass-specific metabolic demands, this tradeoff was optimized through the use of

426 daily torpor (Lovegrove et al., 1999; Lovegrove et al., 2001a, b; Mzilikazi et al., 2002;

427 Mzilikazi and Lovegrove, 2004), which profoundly decreases daily energy demands. Daily

428 torpor is a plesiomorphic characteristic in mammals (Lovegrove, 2012a) and may have been

429 retained throughout the Cenozoic in elephant-shrews to offset the costs of micro-cursoriality.

430   In conclusion, elephant-shrews are unique mammals in terms of their dramatic

431 morphological specializations for fast running speeds relative to similar-sized mammals, and

432 also because they are the only cursors capable of offsetting high locomotor costs through

433 daily heterothermy. Uniquely too, both of these characteristics are plesiomorphic, indicating a

434 long history of micro-cursoriality within the Macroscelidea. We propose that micro-

435 cursoriality evolved in small, ground-dwelling forest macroscelids perhaps as early as the

436 Paleocene, but long before the proliferation of cursoriality in larger mammals during the

437 Miocene.

438

439 **Materials and methods**

440

441 Animals were trapped on the farm NoHeep (30° 02′ S, 17° 59′ E, altitude; 600 – 1000 m), 22

442 km north-east of Kamieskroon, Namaqualand, South Africa, using Elliot traps baited with a

443 mixture of peanut butter and rolled oats during July 2011. These two species of *Elephantulus*

444 are synoptic in this arid, rugged, and highly heterogenous environment in the Kamiesberg

445 mountains (Boyles et al., 2012). The two species were identified on the basis of

446 morphological characters that had been verified with genetic analyses at the same study site

447 (Boyles et al., 2012). Two of the authors of this latter study, Smit and McKechnie, assisted us

448 in the field with species identifications. After measuring body weights and running speeds on

449 the same morning of capture and on the following morning, the animals were released after

450 48 h in the evening at their exact place of capture. The elephant shrews were housed at room

451 temperature in a farm building during captivity in rodent cages provided with paper toweling

452 and a refuge tube. They were provided with water and tinned dog food.

453   Maximum running speeds were obtained by timing animals as they ran down a 30 m

454 tunnel runway erected on a flat section of compacted fine gravel. The tunnel (1.2 m wide, 1.4

455 m high) was formed by U-shaped iron rods (10 mm diameter mild steel) placed every 3 m

456 and covered with 30% green shade cloth. Along the length of the last 30 m of the tunnel, we

457 placed three pairs of colour CCD cameras 3 m apart, each pair facing each other, linked to an

458 eight-channel JPEG2000 digital video recorder. We placed a pile of rocks at the end of the

459 tunnel and released the animals ~ 20 m from the rocks at the opposite end of the tunnel.

460 Typically, the animals froze on release, but once they had orientated themselves and had

461 visually located the rock pile, they ran down the tunnel towards the rock cover. Some animals

462 were induced to start running with hand-clapping. Each animal was tested during two running

463 sessions on two consecutive mornings, and on each occasion the individual completed three

464 runs. Running speeds were calculated from playbacks of video recordings. The success of the

465 runs was varied. In some cased the animals ran well, but stopped running in the middle of the

466 tunnel. In other cases the animals 'bounced' off the side of the shade cloth tunnel or tried to

467 climb the sides of the tunnel. For each individual, the 'best' run, or the MRS, was taken as the

468 fastest, uninterrupted run down the full length of the tunnel.

469 We term our data "maximum running speed" only in the sense that these were the

470 fastest speeds that we measured using our method. Our estimates do not preclude the very

471 real possibility that higher maximum speeds may be measured in elephant-shrews under more

472 natural, free-ranging conditions. We suspect that the local knowledge exploited by elephant-

473 shrews in the employment of their trail systems that they create within their territories

474 (Rathbun, 2009) probably allows them to attain faster maximum running speeds than those

475 that we measured.

476

477 *Maximum running speed*

478 Our running speed and body mass data were compared with those of other mammals obtained

479 from the literature (Garland, 1983a; Hayssen and Lacy, 1985; Robinson and Redford, 1986;

480 Steudel and Beattie, 1993; Iriarte-Diaz, 2002; Lovegrove, 2003; Rojas et al., 2010) (Table 1,

481 supplementary information). There has much discussion about the questionable methods used

482 to measure running speed and hence the quality of the running speed data that have been used

483 in past analyses (see Garland and Janis, 1993). However, Garland (1993) makes the point that

484 it is unlikely that the data are biased in any systemic way and that, given the 'noise' in the

485 data, it is "…perhaps surprising that we are able to show *any* significant correlations…" of

486 MRS with morphological variables. The only species which we discarded from the dataset

487 was that of the saltatorial Merriam's kangaroo rat *Dipodomys merriami*. We have cause to

488 question the unusually high value of the datum, although not necessarily the potentially high

489   MRSs of kangaroo rats *per se*. First, the MRSs of this kangaroo rat were measured when they

490   were released from traps, using a stopwatch (Kenagy, 1973). Thus the estimate is not

491   comparable with MRS obtained more precisely when animals were timed as they ran over a

492   carefully-measured, uniform distance. Second, the MRS of *D. merriami* (31.2 km/h) was

493   double that of the average MRS (16.0 km/h) for three other species of *Dipodomys* in the data

494   set.

495   It became obvious during the preliminary data analysis that elephant-shrews display

496   the most highly-derived, digitigrade cursorial limbs of all mammals smaller than 1 kg. Thus

497   the mammalian running speed model with which to compare elephant-shrews was not

498   intuitively obvious. We argue here that there is only one hypothesis that is reasonably

499   testable, which is simply that the MRS of elephant-shrews exceeds those of mammals of

500   equivalent body size irrespective of limb morphology. The MRSs of *Elephantulus* (40 - 60 g)

501   cannot be compared with those of digitigrade mammals, such as carnivores and lagomorphs

502   (rabbits and hares) which are mostly larger than 1 kg, because their smaller body sizes would

503   require extrapolation of the digitigrade regression models way beyond the lower bounds of

504   the regression data. Indeed, the same argument applies to a comparison with unguligrade

505   mammals although, as we show below, unguligrade mammals do not show the same scaling

506   pattern of MRS with mass compared with other locomotor modes (Iriarte-Diaz, 2002;

507   Lovegrove, 2004). To select the best model with which to test the hypothesis we employed

508   step-wise analyses of the allometric relationship of body mass and maximum running speed

509   in a phylogenetic context.

510   A phylogeny of all of the species used in the comparisons was compiled using

511   Mesquite version 2.74 (Maddison and Maddison, 2009) from a variety of sources (De Walt

512   et al., 1993; Kruckenhauser et al., 1999; Oshida and Masuda, 2000; DeBry and Sagel, 2001;

513   Herron et al., 2004; Steppan et al., 2004; Bininda-Emonds et al., 2007; Bradley et al., 2007;

514   Meredith et al., 2008; Montgelard et al., 2008; Lovegrove, 2012a) (see supplementary

515   information).

516   All statistical analyses were conducted using R version R-3.0.1 (R Core R Core Team,

517   2012). Since strong inflections have been observed in the scaling with body mass of both

518   MRS (Garland, 1983a) and RRS (Iriarte-Diaz, 2002), we used piecewise regression

519   (Crawley, 2007) to establish whether an inflection existed in the relationship between $\log_{10}$

520   MRS and $\log_{10} M_b$. Data for mammals smaller than and equal to the inflection body mass,

521   termed hereafter the small mammal dataset, were used for further analyses because this body

522   size range embraced the elephant-shrew body sizes. Outliers in the regression analysis of the

523   conventional species data of the small mammal data were identified using Cook's Distance

524   (Cook, 1977) calculated from OLS regressions. Evidence of phylogenetic signal was

525   estimated using Pagel's *lambda* (λ) calculated with the R package 'caper' (Nunn, 2011), and

526   with Blomberg *et al*.'s (2003) *K* statistic using the R packages 'picante' (Kembel et al., 2010)

527   and 'ape' (Paradis et al., 2004). OLS and PGLS models were fitted to $\log_{10}$ MRS as a

528   function of $\log_{10}$ M_b using the R package 'caper' (Nunn, 2011).

529   To determine whether MRS is influenced by locomotor mode in the small mammal

530   dataset, we used a multivariate phylogenetic generalized linear model (PGLS) in which the

531   dependent and independent data were first phylogenetically transformed following the

532   method of Garland and Ives (2000) as implemented by Outomuro *et al*. (2013). We created a

533   factor variable ("foot") which coded the data as either plantigrade, lagomorph-like, saltatorial

534   or digitigrade, and then used a standard multivariate MANCOVA.

535   For the small mammal dataset, two PGLS regressions were calculated; a pure

536   Brownian motion PGLS with branch length transformation set to $\lambda = 1$, and a PGLS with

537   Pagel's maximum likelihood estimation of branch lengths. The best fit model was determined

538   as the model with the lowest AIC.

539   To compare the MRS of elephant-shrews with those of similar-sized mammals, we

540   also computed similar PGLS models for the data for mammals smaller than 500 g (n = 52),

541   termed hereafter the plantigrade dataset. This upper body size limit approximates the 95th

542   percentile of the plantigrade body mass frequency distribution and the intersection between

543   the plantigrade and digitigrade distributions (Lovegrove, 2000, 2001).

544

545   *Matatarsal:femur ratios*

546   Metatarsal and femur ratios were measured from animals obtained from the same site that

547   were sacrificed for a genetic study (Boyles et al., 2012). The MT:F data for *Elephantulus*

548   were compared with those for 135 species of mammal obtained from the literature (Garland

549   and Janis, 1993; Steudel and Beattie, 1993; Carrano, 1999) (Table 2, supplementary

550   information). The datum for the giraffe (MT:F ratio = 1.4) was excluded because it was a

551   very large outlier that had a large leverage influence on the unguligrade regressions (see Fig.

552   1). As described earlier for MRS, a phylogeny of the species used in the MT:F ratio analyses

553   was constructed using Mesquite (supplementary information).

554   Initial plots of the relationship between MT:F ratio and $\log_{10}M_b$ revealed obviously

555   dichotomous allometric relationships; one unique to unguligrade mammals (Artiodactyla and

556   Perrisodactyla), and another to non-unguligrade mammals, which in this dataset included

557 Carnivora, Rodentia, Lagomorpha, Lipotyphla, marsupials, and a monotreme. OLS and

558 PGLS regresssions were fitted to the complete dataset, and to the unguligrade and non-

559 unguligrade data separately, as described above for the MRS analyses.

560

561 *Tibofibula outlines*

562 The outlines of the synostosed tibiofibula of an unnamed Nearctic leptictid (Rose, 1999),

563 *Leptictis dakaotensis* (Rose, 2006), (*Apheliscus*) (Zack et al., 2005b), an extant *Rhynchocyon*

564 (Rose, 1999), were digitized from published graphics. The outlines for *Elephantulus rupestris*

565 were digitized from a photograph taken during the measurement of the MT:F ratios.

566

567 **Acknowledgements**

568

577

578

Table 1. Bone dimensions and maximum running speeds of *Elephantulus ruprestris* and *E. edwardii*.

	E. rupestris	*E. edwardii*
Body mass (g)	60.10 ± 5.02 (n = 10)	49.90 ± 4.22 (n = 4)
Femur length (mm)	26.54 ± 0.69 (n = 5)	26.13 ± 0.38 (n = 5)
Metatarsal length (mm)	26.68 ± 1.15 (n = 5)	24.54 ± 1.26 (n= 5)
MT:F	1.067 ± 0.041 (n = 5)	1.075 ± 0.042 (n = 5)
MRS: max absolute running speed (km/h)	23.6 ± 4.8 (n = 10)	19.4 ± 2.2 (n = 4)
MRS range (km/h)	14.4 - 28.8	10.8 – 21.6

579

580

581 **Table 2**. Statistics of various regression models fitted to data sets of metatarsal:femur ratio as

582 a function of $\log_{10}$ body mass (kg).

Statistics	OLS	PGLS Brownian	PGLS ML
All mammals (n = 135)			
Slope	0.073	-0.042	-0.040
P	< 0.001	< 0.01	< 0.01
Intercept	0.479	0.448	0.449
R^2	0.138	0.064	0.057
Pagel's *lambda*	$\lambda = 0$	$\lambda = 1$	$\lambda = 0.964$
AIC	-16.2	-216.6	-221.6
Unguligrade mammals (n = 56)			
Slope	-0.237	-0.124	-0.124
P	< 0.001	< 0.001	< 0.001
Intercept	1.252	0.919	0.919
R^2	0.327	0.193	0.193
Pagel's *lambda*	$\lambda = 0$	$\lambda = 1$	$\lambda = 1$
AIC	-26.2	-81.1	-81.1
Non-unguligrade mammals (n = 79)			
Slope	-0.020	-0.033	-0.031
P	0.029	0.024	< 0.01
Intercept	0.410	0.338	0.357
R^2	0.061	0.064	0.089
Pagel's lambda	$\lambda = 0$	$\lambda = 1$	0.589
AIC	-157.8	-146.7	-177.5

583

584

585   **Table 3**. Statistics of randomization tests used to detect phylogenetic signal (K) (Blomberg et

586   al., 2003) in the data for body mass, maximum running speed, and MT:F ratio.

Trait	N	K	Variance of K	Mean random K	Z	Randomization test probability (p)
[a]Log$_{10}$ M$_b$ for MRS	80	1.328	0.008	.041	8.036	< 0.001
[a]Log$_{10}$ residual MRS	80	0.360	< 0.001	0.001	4.041	< 0.001
[b]Log$_{10}$M$_b$ for MT:F ratio	56	0.482	0.044	0.133	4.055	< 0.001
[b]Log$_{10}$ residual MT:F	56	0.772	0.003	0.015	4.589	< 0.001
[c]Log$_{10}$M$_b$ for MT:F ratio	79	0.580	0.142	0.571	5.688	< 0.001
[c]Log$_{10}$ residual MT:F	79	0.397	0.002	0.004	2.875	< 0.01

587   [a] 80 mammals species < 20 kg, [b]56 unguligrade species, [c]76 non-unguligrade species.

588

589

590

Table 4. Statistics of multivariate MANOVA analyses testing the influence of body mass and locomotor mode on the maximum running speeds of mammals smaller than 20 kg.

Variable	df	SS	MS	F	p
Non-PGLS multivariate MANOVA					
$Log_{10}M_b$	1	4.002	4.002	234.74	< 0.001
Locomotor mode	3	0.613	0.204	11.99	< 0.001
Residuals	75	1.289	0.017		
PGLS multivariate MANOVA					
$Log_{10}M_b$	1	0.144	0.144	28.17	< 0.001
Locomotor mode	2	0.007	0.003	0.66	0.521
Residuals	76	0.388	0.005		

591

592

593   **Table 5**. Statistics of various regression models fitted to the small mammal data set of $\log_{10}$

594   MRS (km/h) as a function of $\log_{10}$ body mass (kg) (n = 80 species).

Statistics	OLS	PGLS Brownian	PGLS ML
Mammals < 20 kg (n = 80), including all locomotor modes except unguligrade			
Slope	0.232	0.150	0.167
Intercept	1.436	1.384	1.393
R^2	0.685	0.255	0.328
Pagel's *lambda*	$\lambda = 0$	1	$\lambda = 0.905$
AIC	-68.44	-87.32	-93.46
Plantigrade mammals < 500 g (n = 52)			
Slope	0.138	0.052	0.138
Intercept	1.305	1.172	1.304
R^2	0.254	0.033	0.254
Pagel's *lambda*	0	1	0
AIC	-77.10	-65.18	-79.10

595

596

597

598

599

600

Table 6. The metatarsal:femur ratios (MT:F) and habitats of extant macroscelids and their putative condylarth Leptictid ancestors.

Species	MT:F	Habitat	Reference
Extant macroscelids			
Elephantulus edwardii	1.08	Open, rocky desert	This study
Elephantulus rupestris	1.07	Open, rocky desert	This study
Elephantulus proboscideus	1.00	Open, desert	(Carrano, 1999; Rathbun, 2009)
Elephantulus rozetti	0.71	Open, rocky desert	(Evans, 1942; Rathbun, 2009)
Elephantulus brachyrhyncus	0.62	Savanna, woodland	(Carrano, 1999)
Petrodromus tetradactylus	0.61	Closed forest	(Evans, 1942; Rathbun, 2009)
Rhynchocyon petersi	0.56	Closed forest	(Carrano, 1999; Rathbun, 2009)
Rhynchocyon cirnei	0.55	Closed forest	(Evans, 1942; Rathbun, 2009)
Leptictida			
Leptictis dakotensis	0.41	Oligocene forests	(Rose, 2006)
Leptictidium	0.47	Eocene forests	(Rose, 2006)
Prodiacodon tauricinerei	0.46	Early Eocene forests	(Rose, 1999)

601

602

References

604

605 **Alroy, J.** (1998). Cope's Rule and the dynamics of body mass evolution in North American fossil
606 mammals. *Sci.* **280**, 731-734.
607 **Alroy, J., Koch, P. L. and Zachos, J. C.** (2000). Global climate change and North American mammalian
608 evolution. *Paleobiology* **26**, 259-288.
609 **Bininda-Emonds, O. R. P., Cardillo, M., Jones, K. E., Macphee, R. D. E., Beck, R. M. D., Grenyer, R.,**
610 **Price, S. A., Vos, R. A., Gittleman, J. L. and Purvis, A.** (2007). The delayed rise of present-day
611 mammals. *Nat.* **446**, 507-512.
612 **Blanckenhorn, W. U.** (2000). The evolution of body size: What keeps organisms small? *Q. Rev. Biol.*
613 **75**, 385-407.
614 **Blomberg, S. P., Garland, T. and Ives, A. R.** (2003). Testing for phylogenetic signal in comparative
615 data: behavioural traits are more labile. *Evol.* **57**, 717-745.
616 **Blomberg, S. P., Lefevre, J. G., Wells, J. A. and Waterhouse, M.** (2012). Independent contrasts and
617 PGLS regression estimators are equivalent. *Syst. Biol.* **61**, 382-391.
618 **Boyles, J. G., Smit, B., Sole, C. L. and McKechnie, A. E.** (2012). Body temperature patterns in two
619 syntopic elephant shrew species during winter. *Comp. Biochem. Physiol. A* **161**, 89-94.
620 **Bradley, R. D., Durish, N. D., Rogers, D. S., Miller, J. R., Engstrom, M. D. and Kilpatrick, C. W.** (2007).
621 Toward a molecular phylogeny for *Peromyscus*: Evidence from mitochondrial cytochrome-b
622 sequences. *J. Mamm.* **88**, 1146-1159.
623 **Butler, P. M.** (1995). Fossil Macroscelidea. *Mammal Rev.* **25**, 3-14.
624 **Carrano, M. T.** (1999). What, if anything, is a cursor? Categories versus continua for determining
625 locomotor habit in mammals and dinosaurs. *J. Zool, Lond.* **247**, 29-42.
626 **Clarke, A. and Pörtner, H.-O.** (2010). Temperature, metabolic power and the evolution of
627 endothermy. *Biol. Rev.* **85**, 703-727.
628 **Cook, R. D.** (1977). Detection of influential observation in linear regression. *Technometrics* **19**, 15-18.
629 **Crawley, M. J.** (2007). The R Book. Sussex, England: John Wiley & Sons Ltd.
630 **De Walt, T. S., Zimmerman, E. G. and Planz, J. V.** (1993). Mitochondrial-DNA phylogeny of species of
631 the *boylii* and *truei* groups of the genus *Peromyscus J. Mamm.* **74**, 352-362.
632 **DeBry, R. W. and Sagel, R. M.** (2001). Phylogeny of Rodentia (Mammalia) inferred from the nuclear-
633 encoded gene IRBP. *Mol. Phyl. Evol.* **19**, 290-301.
634 **Douady, C. J., Catzeflis, F., Raman, J., Springer, M. S. and Stanhope, M. J.** (2003). The Sahara as a
635 vicariant agent, and the role of Miocene climatic events, in the diversification of the mammalian
636 order Macroscelidea (elephant shrews). *Proc. Natl. Acad. Sci. USA* **100**, 8325-8330.
637 **Edwards, E. J., Osborne, C. P., Stromberg, C. A. E., Smith, S. A., Bond, W. J., Christin, P. A., Cousins,**
638 **A. B., Duvall, M. R., Fox, D. L., Freckleton, R. P. et al.** (2010). The origins of C_4 grasslands: Integrating
639 evolutionary and ecosystem science. *Sci.* **328**, 587-591.
640 **Evans, F. G.** (1942). The osteology and relationships of the elephant shrews (Macroscelididae). *B.*
641 *Am. Mus. Nat. Hist.* **80**, 80-125.
642 **Figueirido, B., Janis, C. M., Perez-Claros, J. A., De Renzi, M. and Palmqvist, P.** (2012). Cenozoic
643 climate change influences mammalian evolutionary dynamics. *Proc. Nat. Acad. Sciences, USA* **109**,
644 722-727.
645 **Garland, T.** (1983a). The relation between maximal running speed and body mass in terrestrial
646 mammals. *J. Zool.* **199**, 157-170.
647 **Garland, T.** (1983b). Scaling the ecological cost of transport to body mass in terrestrial mammals.
648 *The American Naturalist* **121**, 571-587.
649 **Garland, T. and Janis, C. M.** (1993). Does metatarsal/femur ratio predict maximal running speed in
650 cursorial mammals? *J. Zool.* **229** 133-151.

651   **Garland, T. and Ives, A. R.** (2000). Using the past to predict the present: confidence intervals for
652   regression equations in phylogenetic comparative methods. *Am. Nat.* **155**, 346-365.
653   **Hayssen, V. and Lacy, R. C.** (1985). Basal metabolic rates in mammals: taxonomic differences in the
654   allometry of BMR and body mass. *Comp. Biochem. Physiol.* **81A**, 741-754.
655   **Hedges, S. B.** (2001). Afrotheria: plate tectonics meets genomics. *P. Natl. Acad. Sci.-Biol.* **98**, 1-2.
656   **Herron, M. D., Castoe, T. A. and Parkinson, C. L.** (2004). Sciurid phylogeny and the paraphyly of
657   Holarctic ground squirrels (*Spermophilus*). *Mol. Phyl. Evol.* **31**, 1015-1030.
658   **Hildebrand, M.** (1974). Analysis of vertebrate structure. New York: John Wiley & Sons.
659   **Hooker, J. J. and Russell, D. E.** (2012). Early Palaeogene Louisinidae (Macroscelidea, Mammalia),
660   their relationships and north European diversity. *Zool. J. Linn. Soc.* **164**, 856-936.
661   **Iriarte-Diaz, J.** (2002). Differential scaling of locomotor performance in small and large terrestrial
662   mammals. *J. Exp. Biol.* **205**, 2897-2908.
663   **Janis, C. M.** (1993). Tertiary mammal evolution in the context of changing climates, vegetation, and
664   tectonic events. *Annu. Rev. Ecol. Syst.* **24**, 467-500.
665   **Janis, C. M. and Wilhelm, P. D.** (1993). Were there mammalian pursuit predators in the Tertiary?
666   Dances with wolf avatars. *J. Mamm. Evol.* **1**, 103-125.
667   **Jardine, P. E., Janis, C. M., Sahney, S. and Benton, M. J.** (2012). Grit not grass: Concordant patterns
668   of early origin of hypsodonty in Great Plains ungulates and Glires. *Palaeogeogr., Palaeoclimatol.,*
669   *Palaeoecol.* **365**, 1-10.
670   **Jones, K. E. and Purvis, A.** (1997). An optimum body size for mammals? Comparative evidence from
671   bats. *Funct. Ecol.* **11**, 751-756.
672   **Kembel, S. W., Cowan, P. D., Helmus, M. R., Cornwell, W. K., Morlon, H., Ackerly, D. D., Blomberg,**
673   **S. P. and Webb, C. O.** (2010). Picante: R tools for integrating phylogenies and ecology. *Bioinformatics*
674   **26**, 1463-1464.
675   **Kenagy, G. J.** (1973). Daily and seasonal patterns of activity and energetics in a heteromyid rodent
676   community. *Ecology* **54(6)**, 1201-1219.
677   **Kruckenhauser, L., Pinsker, W. and Arnold, W.** (1999). Marmot phylogeny revisited: molecular
678   evidence for a diphyletic origin of sociality. *J. Zool. Syst. Evol. Research* **37**, 49-56.
679   **Lovegrove, B. G.** (2000). The zoogeography of mammalian basal metabolic rate. *Am. Nat.* **156**, 201-
680   219.
681   **Lovegrove, B. G.** (2001). The evolution of body armor in mammals: plantigrade constraints of large
682   body size. *Evol.* **55**, 1464-1473.
683   **Lovegrove, B. G.** (2003). The influence of climate on the basal metabolic rate of small mammals: a
684   slow-fast metabolic continuum. *J. Comp. Physiol. B* **173**, 87-112.
685   **Lovegrove, B. G.** (2004). Locomotor mode, maximum running speed and basal metabolic rate in
686   placental mammals. *Physiol. Biochem. Zool.* **77**, 916-928.
687   **Lovegrove, B. G.** (2012a). The evolution of endothermy in Cenozoic mammals: A plesiomorphic-
688   apomorphic continuum. *Biol. Rev.* **87**, 128-162.
689   **Lovegrove, B. G.** (2012b). The evolution of mammalian body temperature: the Cenozoic
690   supraendothermic pulses. *J. Comp. Physiol. B* **182**, 579-589.
691   **Lovegrove, B. G. and Haines, L.** (2004). The evolution of placental mammal body sizes: Evolutionary
692   history, form, and function. *Oecol.* **138**, 13-27.
693   **Lovegrove, B. G. and Mowoe, M. O.** (2013). The evolution of mammal body sizes: responses to
694   Cenozoic climate change in North American mammals. *J. Evol. Biol.* **26**, 1317-1329.
695   **Lovegrove, B. G., Lawes, M. J. and Roxburgh, L.** (1999). Confirmation of pleisiomorphic daily torpor
696   in mammals: the round-eared elephant shrew *Macroscelides proboscideus* (Macroscelidea). *J.*
697   *Comp. Physiol. B* **169**, 453-460.
698   **Lovegrove, B. G., Raman, J. and Perrin, M. R.** (2001a). Heterothermy in elephant shrews,
699   *Elephantulus* spp. (Macroscelidea): daily torpor or hibernation? *J. Comp. Physiol. B* **171**, 1-10.
700   **Lovegrove, B. G., Raman, J. and Perrin, M. R.** (2001b). Daily torpor in elephant shrews
701   (Macroscelidea: *Elephantulus* spp.) in response to food deprivation. *J. Comp. Physiol. B* **171**, 11-21.

702 **MacFadden, B. J.** (2000). Cenozoic mammalian herbivores from the Americas: Reconstructing
703 ancient diets and terrestrial communities. *Annu. Rev. Ecol. Syst.* **31**, 33-59.
704 **Maddison, W. P. and Maddison, D. R.** (2009). Mesquite: a modular system for evolutionary analysis.
705 Version 1.12.
706 **Meredith, R. W., Westerman, M. and Springer, M. S.** (2008). A phylogeny and timescale for the
707 living genera of kangaroos and kin (Macropodiformes : Marsupialia) based on nuclear DNA
708 sequences. *Aust. J. Zool.* **56**, 395-410.
709 **Montgelard, C., Forty, E., Arnal, V. and Matthee, C. A.** (2008). Suprafamilial relationships among
710 Rodentia and the phylogenetic effect of removing fast-evolving nucleotides in mitochondrial, exon
711 and intron fragments. *BMC Evol. Biol.* **8**, 231.
712 **Mzilikazi, N. and Lovegrove, B. G.** (2004). Daily torpor in free-ranging rock elephant shrews,
713 *Elephantulus myurus* : a year-long study. *Physiol. Biochem. Zool.* **77**, 285-296.
714 **Mzilikazi, N., Lovegrove, B. G. and Ribble, D. O.** (2002). Exogenous passive heating during arousal in
715 free-ranging rock elephant shrews, *Elephantulus myurus*. *Oecol.* **133**, 307-314.
716 **Nunn, C.** (2011). The comparative approach in evolutionary anthropology and biology. Cicago:
717 University of Cicago Press.
718 **O'Leary, M. A., Bloch, J. I., Flynn, J. J., Gaudin, T. J., Giallombardo, A., Giannini, N. P., Goldberg, S.**
719 **L., Kraatz, B. P., Luo, Z. X., Meng, J. et al.** (2013). The placental mammal ancestor and the post-K-Pg
720 radiation of placentals. *Sci.* **339**, 662-667.
721 **Oshida, T. and Masuda, R.** (2000). Phylogeny and zoogeography of six squirrel species of the genus
722 *Sciurus* (Mammalia, Rodentia), inferred from cytochome b gene sequences. *Zool.Sci.* **17**, 405-409.
723 **Outomuro, D., Adams, D. C. and Johansson, F.** (2013). Evolution of wing shape in ornamented-
724 winged damselflies. *Evolutionary Biology* **(in press)**.
725 **Paradis, E., Claude, J. and Strimmer, K.** (2004). APE: Analyses of Phylogenetics and Evolution in R
726 language. *Bioinformatics* **20**, 289-290.
727 **R Core Team.** (2012). R: A language and environment for statistical computing. In *R Foundation for*
728 *Statistical Computing, Vienna, Austria (http://www.R-project.org)*.
729 **Rathbun, G. B.** (1979). The social structure and ecology of elephant-shrews. Berlin: Paul Parey.
730 **Rathbun, G. B.** (2009). Why is there discordant diversity in sengi (Mammalia: Afrotheria:
731 Macroscelidea) taxonomy and ecology? *Afr. J. Ecol.* **47**, 1-13.
732 **Robinson, J. G. and Redford, K. H.** (1986). Body size, diet, and population density of Neotropical
733 forest mammals. *Am. Nat.* **128**, 665-680.
734 **Rojas, A. D., Körtner, G. and Geiser, F.** (2010). Do implanted transmitters affect maximum running
735 speed of two small marsupials? *J. Mamm.* **91**, 1360-1364.
736 **Rookmaker, L. C.** (1989). The Zoological Exploration of Southern Africa. Rotterdam: A.A. Balkema.
737 **Rose, K. D.** (1999). Postcranial skeleton of Eocene Leptictidae (Mammalia), and its implications for
738 behavior and relationships. *J. Vert. Paleontol.* **19**, 355-372.
739 **Rose, K. D.** (2006). The postcranial skeleton of early Oligocene *Leptictis* (Mammalia: Leptictida), with
740 a preliminary comparison to *Leptictidium* from the middle Eocene of Messel. *Palaeontgr. Ab. A* **278**,
741 37-56.
742 **Secord, R., Bloch, J. I., Chester, S. G. B., Boyer, D. M., Wood, A. R., Wing, S. L., Kraus, M. J.,**
743 **McInerney, F. A. and Krigbaum, J.** (2012). Evolution of the earliest horses driven by climate change
744 in the Paleocene-Eocene Thermal Maximum. *Sci.* **335**, 959-962.
745 **Smit, H. A., van Vuuren, B. J., O'Brien, P. C. M., Ferguson-Smith, M., Yang, F. and Robinson, T. J.**
746 (2011). Phylogenetic relationships of elephant-shrews (Afrotheria, Macroscelididae). *J. Zool.* **284**,
747 133-143.
748 **Smith, F. A. and Lyons, S. K.** (2011). How big should a mammal be? A macroecological look at
749 mammalian body size over space and time. *Phil. Trans. Roy. Soc. Lond. B* **366**, 2364-2378.
750 **Springer, M. S., Cleven, G. C., Madsen, O., de Jong, W. W., Waddell, V. G., Amrine, H. M. and**
751 **Stanhope, M. J.** (1997). Endemic African mammals shake the phylogenetic tree. *Nat.* **388**, 61-64.

752 **Stanhope, M. J., Waddell, V. G., Madsen, O., de Jong, W. W., Hedges, S. B. and Cleven, G. C.** (1998).
753 Molecular evidence for multiple origins of Insectivora and for a new order of endemic African
754 insectivorous mammals. *Proc.Nat.Acad.Sci.Usa* **95**, 9972.
755 **Stein, B. R. and Casinos, A.** (1997). What is a cursorial mammal? *J. Zool.* **242**, 185-192.
756 **Steppan, S. J., Adkins, R. M. and Anderson, J.** (2004). Phylogeny and divergence-date estimates of
757 rapid radiations in muroid rodents based on multiple nuclear genes. *Syst. Biol.* **53** 533-553.
758 **Steudel, K. and Beattie, J.** (1993). Scaling of cursoriality in mammals. *J. Morphol.* **217**, 55-63.
759 **Tabuce, R., Coiffait, B., Coiffait, P. E., Mahboubi, M. and Jaeger, J. J.** (2001). A new genus of
760 Macroscelidea (Mammalia) from the Eocene of Algeria: A possible origin for elephant-shrews. *J. Vert.*
761 *Paleontol.* **21**, 535-546.
762 **Tabuce, R., Marivaux, L., Adaci, M., Bensalah, M., Hartenberger, J. L., Mahboubi, M., Mebrouk, F.,**
763 **Tafforeau, P. and Jaeger, J. J.** (2007). Early tertiary mammals from north Africa reinforce the
764 molecular Afrotheria clade. *Proc. R. Soc. B* **274**, 1159-1166.
765 **Taylor, C. R., Schmidt-Nielsen, K. and Raab, J. L.** (1970). Scaling of energetic cost of running to body
766 size in mammals. *American Journal of Physiology* **219**, 1104-1107.
767 **Thewissen, J. G. M.** (1990). Evolution of Paleocene and Eocene Phenacodontidae (Mammlia,
768 Condylarthra). *University of Mitchican Papers on Paleotology* **29**, 1-120.
769 **Van Damme, R. and Van Dooren, T. J. M.** (1999). Absolute versus per unit body length speed of prey
770 as an estimator of vulnerability to predation. *Anim. Behav.* **57**, 347-352.
771 **Yuanqing, W., Jin, M., Xijun, N. and Chuankui, L.** (2007). Major events of Paleogene mammal
772 radiation in China. *Geol. J.* **42**, 415-430.
773 **Zack, S. P., Penkrot, T. A., Krause, D. W. and Maas, M. C.** (2005a). A new apheliscine "condylarth"
774 mammal from the late Paleocene of Montana and Alberta and the phylogeny of "hyopsodontids'.
775 *Acta Palaeontol. Pol.* **50**, 809-830.
776 **Zack, S. P., Penkrot, T. A., Bloch, J. I. and Rose, K. D.** (2005b). Affinities of 'hyopsodontids' to
777 elephant shrews and a Holarctic origin of Afrotheria. *Nat.* **434**, 497-501.
778

779 **Figure legends**

780

781 **Figure 1**

782 The metatarsal:fermur ratios (MT:F) of 135 mammal species plotted as function of $\log_{10}$ body

783 mass. The red line is the PGLS regression line for the combined dataset, whereas the black

784 and the blue lines are the PGLS regression lines for the separate unguligrade and non-

785 unguligrade datasets, respectively. The red arrow indicates the evolutionary trend of

786 decreased body size and increased MT:F ratios that occurred in open habitat *Elephantulus*

787 species during Miocene aridification.

788

789 **Figure 2**

790 The maximum running speed as a function of body mass of 143 mammal species. The

791 vertical dashed line indicates a significant inflection at 20 kg separating the allometries of the

792 MRS of small and large mammals.

793

794 **Figure 3**

795 Maximum running speed as a function of body mass for 80 mammals < 20 kg. The regression

796 line (solid line) and the 95% confidence (short dashed lines) and prediction (long dashed

797 lines) intervals were obtained from a Brownian Motion PGLS model, equivalent to an OLS

798 regression of the phylogenetically independent linear contrasts (see Table 4 for regression

799 statistics).

800

801 **Figure 4**

802 Maximum running speed as a function of body mass of 52 mammals < 500 g. The regression

803 line (solid line) and the 95% confidence (long dashed lines) and prediction (short dashed

804 lines) intervals were obtained from an OLS regression model (see Table 4 for regression

805 statsitics).

806

807 **Figure 5**

808 A working model of the phylogeny of the Macroscelidae and their leptictid ancestors. The

809 topology of the basal macroscelids follows Hooker and Russel (2012), Zack et al (2005b;

810 2005a), Butler (1995) and Tabuce et al (2001), whereas that of the traditionally recognized

811 macroscelid families follows Tabuce et al (2007) and Smit et al (2011). Note that the

812   Aphelisidae have recently been recognized as North American ungulates basal to Euungulata

813   (= crown Perrisodactyla and Artiodactyla) and not as macroscelids.

814

815   **Figure 6**.

816   Digitized outlines of the synostosed tibiofibula of an unnamed Nearctic leptictid (Rose,

817   1999), *Leptictis dakaotensis* (Rose, 2006), (*Apheliscus*) (Zack et al., 2005b), an extant

818   *Rhynchocyon* (Rose, 1999), and *Elephantulus rupestris* (this study).The degree of distal

819   synostosis (fusion) is indicative of increased cursorial capacity. Not to scale, but all limbs are

820   scaled to the same length.

821

822

823 **Supporting information**

824

825 **Figure 1 S1. Body temperatures**

826 **Appendix S1. Phylogeny for maximum MT:F ratio (n = 135)**

827 **Appendix S2. Phylogeny for maximum running speed (n = 80)**

828 **Table 1 S1. Maximum running speed and body mass data**

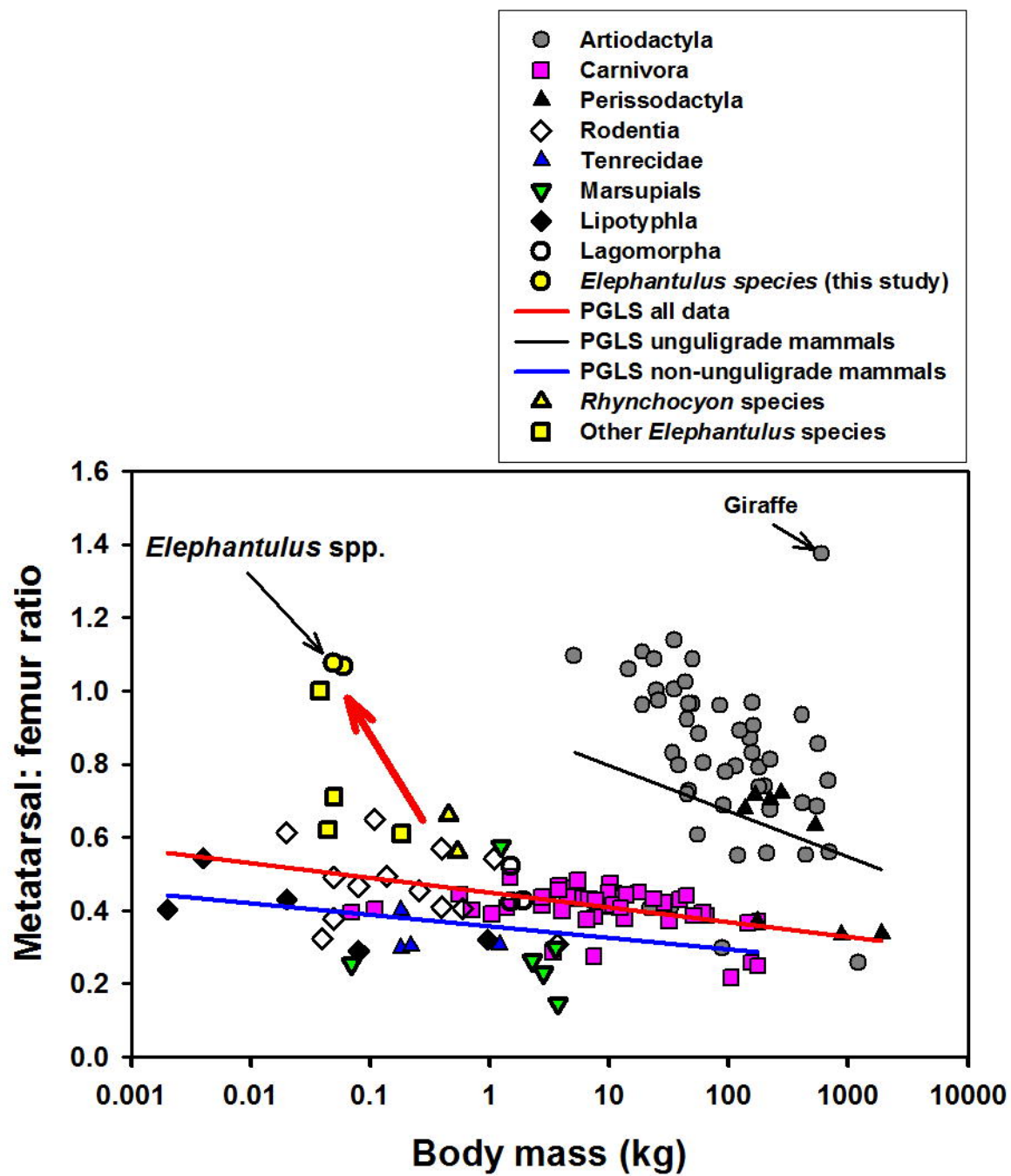829 **Table 2 S2. Body mass and metatarsal:femur ratio data**
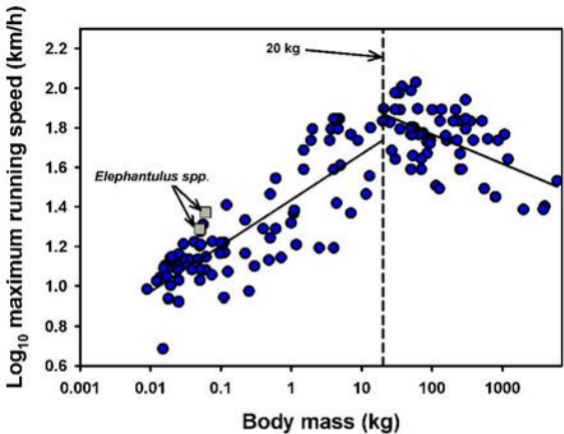
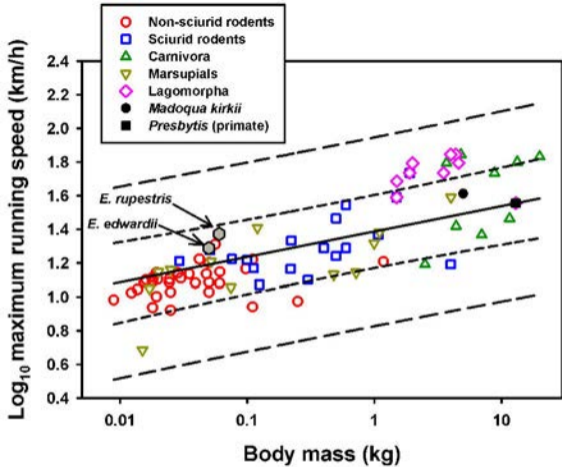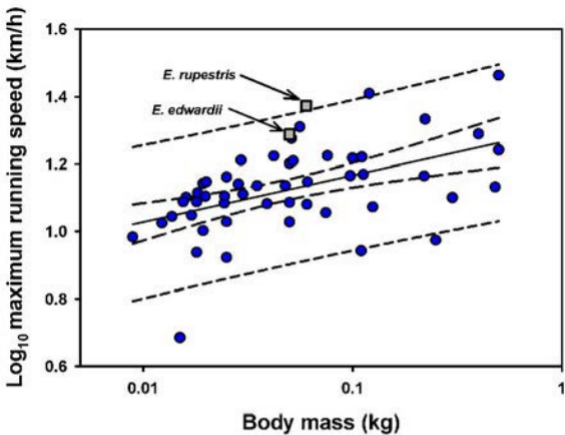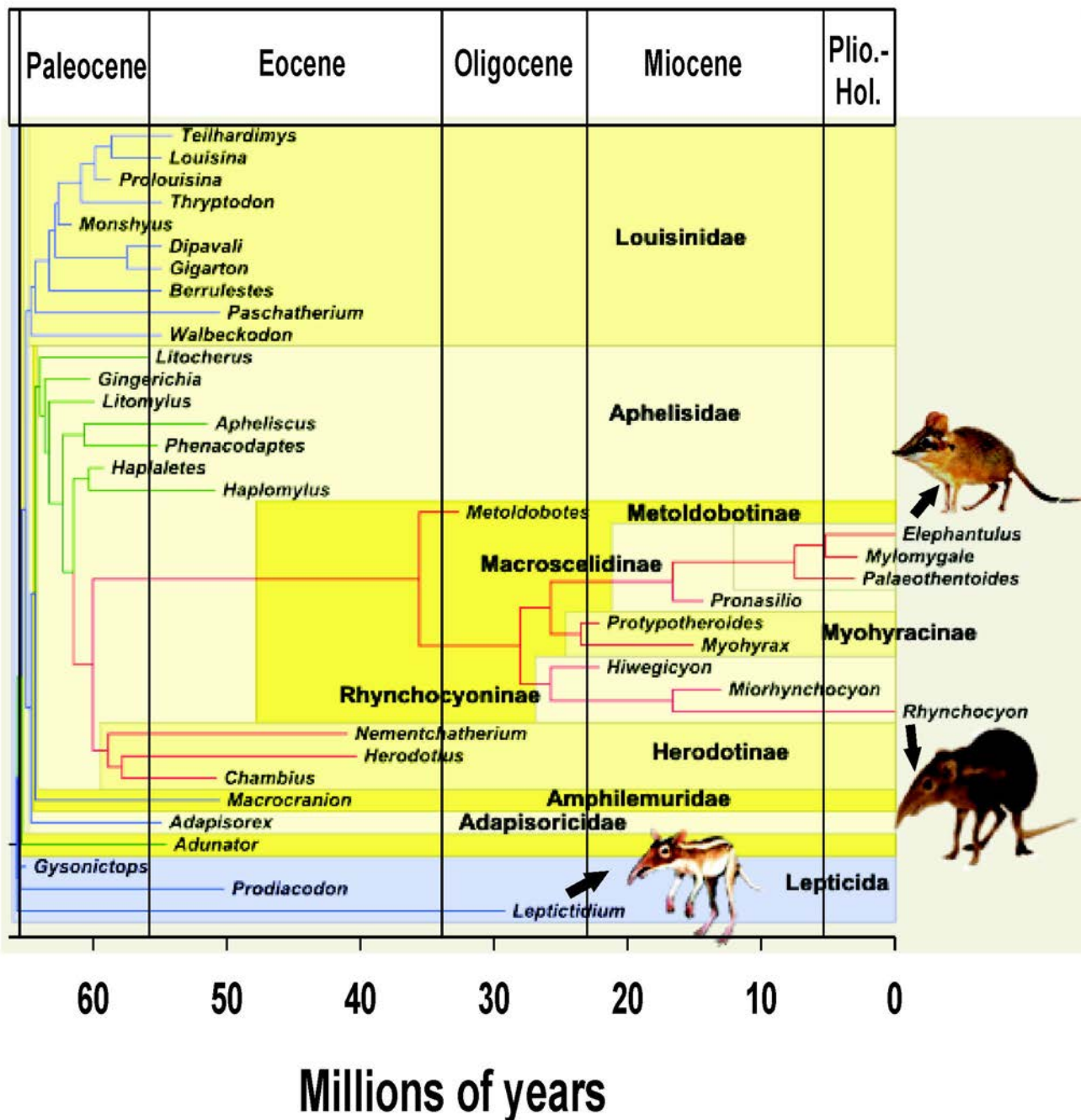830

Figure 1

Figure 2: Lovegrove and Mowoe

Figure 3

Figure 4

Paleocene	Eocene	Oligocene	Miocene	Plio.-Hol.

Teilhardimys
Louisina
Prolouisina
Thryptodon
Monshyus
Dipavali
Gigarton
Berrulestes
Paschatherium
Walbeckodon

Louisinidae

Litocherus
Gingerichia
Litomylus
Apheliscus
Phenacodaptes
Haplaletes
Haplomylus

Aphelisidae

Metoldobotes

Metoldobotinae

Elephantulus
Mylomygale
Palaeothentoides

Macroscelidinae

Pronasilio
Protypotheroides
Myohyrax

Myohyracinae

Hiwegicyon
Miorhynchocyon

Rhynchocyoninae

Rhynchocyon

Nementchatherium
Herodotius
Chambius

Herodotinae

Macrocranion

Amphilemuridae

Adapisorex

Adapisoricidae

Adunator

Gysonictops

Prodiacodon

Lepticida

Leptictidium

60	50	40	30	20	10	0

Millions of years

Eocene Nearctic Leptictid   *Leptictis dakotensis*   *Apheliscus*   *Rhynchocyon*   *Elephantulus rupestris*